

**TECHNICAL EVALUATION OF THE GE ESSENTIAL
FULL FIELD DIGITAL MAMMOGRAPHY SYSTEM**

NHSBSP Equipment Report 0803

May 2008

**K C Young, J M Oduko, O Gundogdu and A Alsager
National Coordinating Centre for the Physics of Mammography**

Enquiries

Enquiries about this report should be addressed to:

Professor KC Young

National Coordinating Centre for the Physics of Mammography

Medical Physics Department

Royal Surrey County Hospital

Guildford

GU2 7XX

Tel: 01483 406738

Fax: 01483 406742

Email: ken.young@nhs.net

Published by

NHS Cancer Screening Programmes

Fulwood House

Old Fulwood Road

Sheffield

S10 3TH

Tel: 0114 271 1060

Fax: 0114 271 1089

Email: info@cancerscreening.nhs.uk

Website: www.cancerscreening.nhs.uk

© NHS Cancer Screening Programmes 2008

The contents of this document may be copied for use by staff working in the public sector but may not be copied for any other purpose without prior permission from the NHS Cancer Screening Programmes.

The report is available in PDF format on the NHS Cancer Screening Programmes' website.

Typeset by Prepress Projects Ltd, Perth (www.prepress-projects.co.uk)

Printed by Henry Ling Limited

CONTENTS

ACKNOWLEDGEMENTS	iv
1. INTRODUCTION	1
1.1 Testing procedures and performance standards for digital mammography	1
1.2 Objectives	1
2. METHODS	1
2.1 System tested	1
2.2 Detector response	2
2.3 Dose measurement	2
2.4 Contrast to noise ratio	3
2.5 Noise analysis	4
2.6 Image quality measurements	5
2.7 Optimisation	6
3. RESULTS	7
3.1 Detector response	7
3.2 AEC performance	8
3.3 Noise measurements	12
3.4 Image quality measurements	13
3.5 Comparison with other systems	16
3.6 Optimisation	20
4. DISCUSSION	22
5. CONCLUSIONS	23
6. MANUFACTURER'S COMMENT	23
REFERENCES	23

ACKNOWLEDGEMENTS

The authors are grateful to the staff at Princess Grace Hospital, London, for their help in evaluating the unit at their site.

1. INTRODUCTION

1.1 Testing procedures and performance standards for digital mammography

This report is one of a series evaluating commercially available digital mammography systems on behalf of the NHS Breast Screening Programme (NHSBSP). The testing methods and standards applied are mainly derived from NHSBSP Equipment Report 0604.¹ This is referred to in this document as the NHSBSP protocol and it has the same image quality and dose standards as those provided in the European protocol.^{2,3} The European protocol was followed where there is a more detailed performance standard, eg for the automatic exposure control (AEC) system.

1.2 Objectives

The purpose of these tests was to determine whether this system meets the main standards in the NHSBSP and European protocols and to provide performance data for comparison against other manufacturers' products. Additional measurements were also undertaken to assess how well the system's AEC was optimised. The method of assessing optimisation has been reported previously.^{4,5} Clinical evaluations are published separately by the NHSBSP where systems meet the minimum standards in the NHSBSP protocol. A final decision on the suitability of systems for use in the NHSBSP depends on a review of both the technical and clinical evaluations.

2. METHODS

2.1 System tested

The tests were conducted at the Princess Grace Hospital, London, on the system shown in Figure 1 and described in Table 1. The system is a development of the technology used in the GE Senographe DS. The most obvious change is the increased size of the detector. However, there have been a number of other changes designed to optimise the efficiency of the system.

Table 1 System description

Target materials	Molybdenum and rhodium
Added filtration	30 μm molybdenum 25 μm rhodium
Pixel size	100 μm (in detector plane)
Detector area	24 \times 31 cm
Pixel array	2400 \times 3070
AEC modes	Standard, dose, contrast



Figure 1 Photo of GE Essential.

2.2 Detector response

The detector response was measured broadly as described in the NHSBSP protocol. A phantom of perspex (PMMA) with a total thickness of 45 mm was positioned at the tube exit port and exposed using the three target/filter combinations available (Mo/Mo, Mo/Rh and Rh/Rh) at tube voltages spanning the range used clinically (25, 28, 31 and 34 kV). An ion chamber was positioned at the surface of the breast support table, and the entrance surface air kerma measured for a single tube current-time product for each tube voltage and target/filter combination tested. The readings were corrected to the surface of the imaging detector using the inverse square law. It was determined that the imaging detector is at a distance of 660 mm from the tube focus and 5 mm below the protective cover. No correction was made for attenuation by the protective plates above the detector but the grid was removed. The images were saved as unprocessed files and transferred to another computer for analysis. A 10 mm square region of interest (ROI) was positioned on the midline and 6 cm from the chest wall edge of each image. The average pixel value and the standard deviation of pixel values within that region were measured. The relationship between average pixel values and the detector entrance surface air kerma was determined. The magnitude of the pixel offset at zero air kerma was determined.

2.3 Dose measurement

Doses were measured by using the AEC in each of its three dose modes to expose different thicknesses of PMMA, with an area of 18 × 24 cm. Small rigid expanded polystyrene spacers were added at the edge of the test object to adjust the total thickness to be equal to the equivalent breast thickness. Mean glandular doses (MGDs) were calculated for the equivalent breast thicknesses and the displayed doses recorded. To measure the contrast-to-noise ratio (CNR) an aluminium square, 10 mm × 10 mm, and 0.2 mm thick was placed on top

of a 20 mm thick block, with one edge on the midline and 6 cm from the chest wall edge. Additional layers of PMMA were added on top to vary the total thickness.

2.4 Contrast to noise ratio

The images of the blocks of PMMA obtained during the dose measurement were analysed to obtain the CNRs. Twenty small square ROIs (approximately 2.5 mm × 2.5 mm) were used to determine the average signal and the standard deviations in the signal within the image of the aluminium square (4 ROIs) and the surrounding background (16 ROIs), as shown in Figure 2. Small ROIs are used to minimise distortions due to the heel effect. However, this is less important for this system because flat-field correction is applied. The CNR was calculated for each image as defined in the NHSBSP and European protocols.

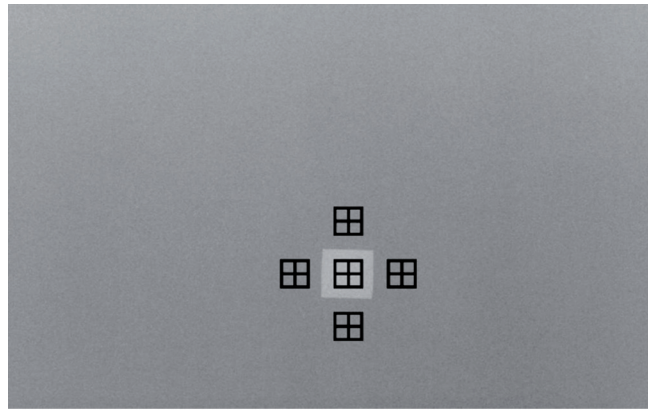


Figure 2 Location and size of ROI used to determine the CNR.

To apply the standards in the European protocol the limiting value for CNR (using 50 mm PMMA) was determined according to equation 1. This equation determines the CNR value ($CNR_{limiting\ value}$) that is necessary to achieve the minimum threshold gold thickness for the 0.1 mm detail (i.e. $threshold\ gold_{limiting\ value} = 1.68\ \mu m$ which is equivalent to $threshold\ contrast_{limiting\ value} = 23.0\%$ using 28 kV Mo/Mo). Threshold contrasts were calculated as described in the European protocol and used in equation 1.

$$CNR_{limiting\ value} = CNR_{measured} \times \frac{TC_{measured}}{TC_{limiting\ value}} \quad (1)$$

The relative CNR was then calculated according to equation 2 and compared with the limiting values provided for relative CNR shown in Table 2. The minimum CNR required to meet this criterion was then calculated.

$$Relative\ CNR = CNR_{measured} / CNR_{limiting\ value} \quad (2)$$

Table 2 Limiting values for relative CNR

Thickness of PMMA (mm)	Equivalent breast thickness (mm)	Limiting values for relative CNR (%) in European protocol
20	21	>115
30	32	>110
40	45	>105
45	53	>103
50	60	>100
60	75	>95
70	90	>90

2.5 Noise analysis

The 45 mm thick block of PMMA with aluminium square used for the measurement of CNR was exposed using manually selected tube loading across the range available. The kV target/filter combination used was that selected by the AEC in standard dose mode. The compression paddle was in place. The same regions of interest used in the CNR measurement were applied to the corresponding unprocessed images. The average standard deviations of the pixel values in the background ROI for each image were used to investigate the relationship between dose to the detector and image noise. It was assumed that this noise comprises three components – electronic noise, structural noise and quantum noise – with the relationship shown in equation 3. This method of analysis has been described previously.⁵

$$\sigma_p = \sqrt{k_e^2 + k_q^2 p + k_s^2 p^2} \quad (3)$$

where σ_p is the standard deviation in pixel values within an ROI with a uniform exposure and a mean pixel value p , and k_e , k_q and k_s are the coefficients determining the amount of electronic, quantum and structural noise in a pixel with a value p . For simplicity, the noise is generally presented here as relative noise defined as in equation 4.

$$\text{Relative noise} = \frac{\sigma_p}{p} \quad (4)$$

The variation in relative noise with mean pixel value was evaluated and fitted using equation 3, and non-linear regression used to determine the best fit for the constants and their asymptotic confidence limits (using Graphpad Prism Version 4.03 for Windows, Graphpad software, San Diego, CA, USA; www.graphpad.com). This established whether the experimental measurements of the noise fitted this equation, and the relative proportions of the different noise components. In fact the relationship between noise and pixel values has been found empirically to be approximated by a simple power relationship, as shown in equation 5.

$$\frac{\sigma_p}{p} = k_t p^{-n} \quad (5)$$

where k_l is a constant. If the noise were purely quantum noise the value of n would be 0.5. However, the presence of electronic and structural noise means that n can be slightly higher or lower than 0.5.

2.6 Image quality measurements

Contrast detail measurements were made using the CDMAM phantom (version 3.4, UMC St. Radboud, Nijmegen University, Netherlands). The phantom was positioned with a 20 mm thickness of PMMA above and below, to give a total attenuation approximately equivalent to 50 mm of PMMA or 60 mm thickness of typical breast tissue. This arrangement was imaged using the x-ray set's AEC in standard mode with small rigid expanded polystyrene spacers in place to create a total thickness of 60 mm. This procedure was repeated with small adjustments to the phantom position to obtain a representative sample of 16 images at this dose level. Unprocessed images were transferred to disk for subsequent analysis off-site. Further images of the test phantom were then obtained at other dose levels by manually selecting higher and lower mAs values with the same beam quality as selected under AEC control.

An automatic method of reading the CDMAM images was used.⁶⁻⁸ The threshold gold thickness for a typical human observer was predicted using equation 6.

$$TC_{predicted} = rTC_{auto} \quad (6)$$

where $TC_{predicted}$ is the predicted threshold contrast for a typical observer and TC_{auto} is the threshold contrast measured using an automated procedure with CDMAM images. Contrasts were calculated from gold thickness for a nominal tube voltage of 28 kV and a Mo/Mo target/filter combination as described in the European protocol. r is the average ratio between human and automatic threshold contrast determined experimentally with the values shown in Table 3.⁶

Table 3 Values of r used to predict threshold contrast

Diameter of gold disc (mm)	Average ratio of human to automatically measured threshold contrast (r)
0.08	1.40
0.10	1.50
0.13	1.60
0.16	1.68
0.20	1.75
0.25	1.82
0.31	1.88
0.40	1.94
0.50	1.98
0.63	2.01
0.80	2.06
1.00	2.11

The main advantage of automatic reading is that it has the potential of eliminating observer error, which is a significant problem when using human observers. However, it should be noted that at the present time the official protocols are based on human reading.

The predicted threshold gold thickness for each detail diameter at each dose level was fitted with a curve as described in the NHSBSP protocol. The confidence limits for the predicted threshold gold thicknesses have been previously determined by a resampling method using a large set of images. The threshold contrasts quoted in the tables of results are derived from the fitted curves, as this has been found to improve the accuracy.⁶

The expected relationship between threshold contrast and dose is shown in equation 7.

$$\text{Threshold contrast} = \lambda D^{-n} \quad (7)$$

D represents the MGD for a 60 mm thick standard breast equivalent to the test phantom configuration used for the image quality measurement. λ is a constant to be fitted. It is assumed that a similar equation applies when using threshold gold thickness instead of contrast. This equation was plotted with the experimental data for each detail size from 0.1 to 1.0 mm. The value of n having the best fit to the experimental data was determined.

2.7 Optimisation

A method for determining optimal beam qualities and exposure factors for digital mammography systems has been described previously and was used to evaluate this system.^{4,5} CNR and mean glandular dose were measured as described above using blocks of PMMA from 20 to 70 mm thick. For each thickness, up to five tube voltage settings were used (25, 28, 31, 34 and 37 kV) with each of the target/filter combinations available and the mAs recorded. The MGDs to typical breasts with attenuation equivalent to each thickness of the PMMA were calculated as described in the NHSBSP protocol. Each exposure was designed to achieve a standard pixel value. Additional CNR measurements were made with a 45 mm thickness of PMMA using the AEC selected beam quality and a wide range of manually selected mAs values. The relationship between noise and pixel values in digital mammography systems has been previously⁵ shown to be approximated by:

$$\text{Relative noise} = \frac{\sqrt{\frac{sd(bgd)^2 + sd(Al)^2}{2}}}{p} = k_i p^{-n} \quad (8)$$

where k_i is a constant, and p is the average background pixel value linearised with absorbed dose to the detector. $sd(bgd)$ is the average standard deviation of pixel values in the ROIs over the background. $sd(Al)$ is the average standard deviation of pixel values in an ROI over a 0.2 mm × 10 mm × 10 mm piece of aluminium. The value of n was found by fitting this equation to the experimental data. Equation 9 was then used to calculate the dose required to achieve a target CNR, where k is a constant to be fitted and D is the MGD for a breast of equivalent thickness.

$$\text{CNR} = kD^n \quad (9)$$

The target CNR was that calculated to reach either the minimum or achievable image quality in the NHSBSP and European protocols using the following relationship.

$$\text{Threshold contrast} = \frac{\lambda}{\text{CNR}} \quad (10)$$

where λ is a constant that is independent of dose, beam quality and the thickness of attenuating material. The optimal beam quality for each thickness was selected as that necessary to achieve the target CNR for the minimum dose.

3. RESULTS

3.1 Detector response

The detector was found to have a linear response as shown in Figure 3. The gradient was measured to be 0.111 μGy per pixel value at 29 kV Rh/Rh. The exposures selected by the AEC resulted in average pixel values in the range of 300–1000 depending on the mode selected, and the simulated breast thickness. A standard value of 600 was chosen to determine the reference entrance air kerma, which was 66.8 μGy using 29 kV Rh/Rh. The corresponding reference entrance air kermas to produce pixel values of 600 using other beam qualities are shown in Figure 4.

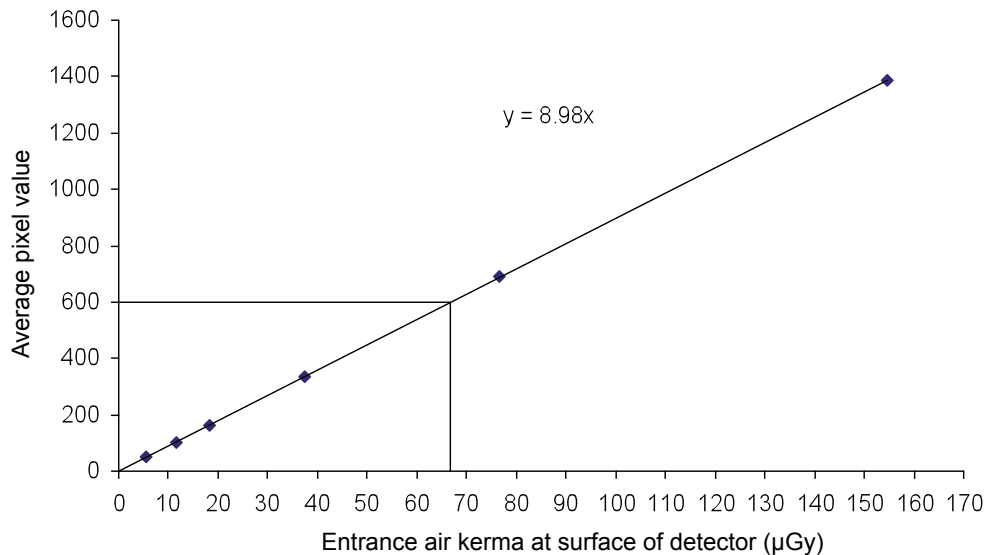


Figure 3 Detector response.

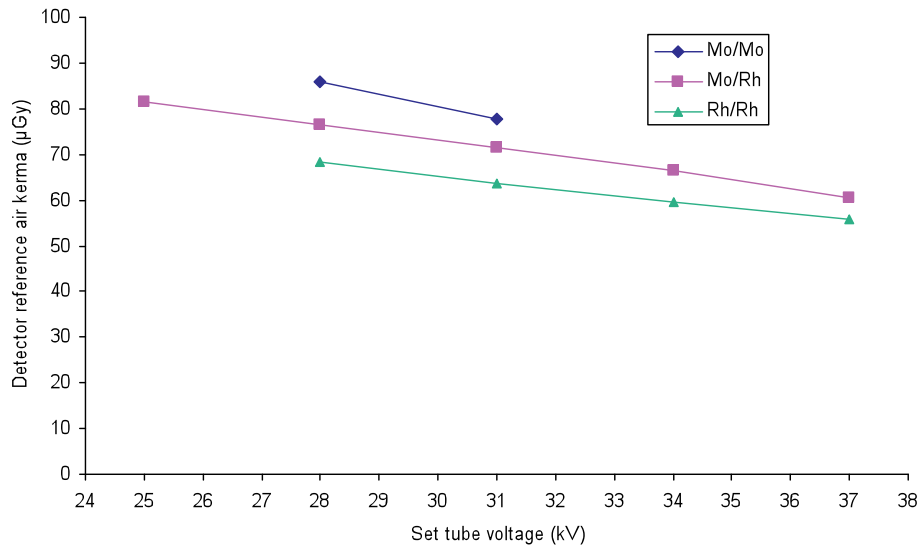


Figure 4 Detector reference air kerma for a pixel value of 600.

3.2 AEC performance

3.2.1 Dose

The mean glandular doses for breasts simulated with PMMA exposed under AEC control are shown in Table 4 and Figure 5 for the three AEC modes available. At all thicknesses the dose was below the remedial level in the NHSBSP protocol, which is the same as the maximum acceptable level in the European protocol.

Table 4a Mean glandular dose for simulated breasts (AEC in standard mode)

PMMA thickness (mm)	Equivalent breast thickness (mm)	kV	Target	Filter	mAs	MGD (mGy)	Displayed dose (mGy)	NHSBSP remedial level (mGy)
20	21	26	Mo	Mo	25.9	0.66	0.78	>1.0
30	32	26	Mo	Mo	47.1	0.91	1.11	>1.5
40	45	29	Rh	Rh	41.1	0.93	1.17	>2.0
45	53	29	Rh	Rh	48.6	1.01	1.33	>2.5
50	60	29	Rh	Rh	57.7	1.10	1.46	>3.0
60	75	29	Rh	Rh	81.3	1.36	1.81	>4.5
70	90	30	Rh	Rh	81.3	1.35	1.94	>6.5

Technical evaluation of the GE Essential FFDM system

Table 4b Mean glandular dose for simulated breasts (AEC in dose mode)

PMMA thickness (mm)	Equivalent breast thickness (mm)	kV	Target	Filter	mAs	MGD (mGy)	Displayed dose (mGy)	NHSBSP remedial level (mGy)
20	21	26	Mo	Mo	13.0	0.38	0.48	> 1.0
30	32	26	Mo	Mo	27.3	0.53	0.66	> 1.5
40	45	29	Rh	Rh	30.1	0.68	0.87	> 2.0
45	53	29	Rh	Rh	35.4	0.73	1.00	> 2.5
50	60	29	Rh	Rh	44.0	0.84	1.14	> 3.0
60	75	30	Rh	Rh	53.4	1.01	1.39	> 4.5
70	90	30	Rh	Rh	81.6	1.35	1.97	.5

Table 4c Mean glandular dose for simulated breasts (AEC in contrast mode)

PMMA thickness (mm)	Equivalent breast thickness (mm)	kV	Target	Filter	mAs	MGD (mGy)	Displayed dose (mGy)	NHSBSP remedial level (mGy)
20	21	26	Mo	Mo	31.2	0.80	0.91	> 1.0
30	32	26	Mo	Mo	63.2	1.22	1.46	> 1.5
40	45	29	Rh	Rh	65.1	1.45	1.80	> 2.0
45	53	29	Rh	Rh	74.9	1.55	1.98	> 2.5
50	60	29	Rh	Rh	90.7	1.74	2.23	> 3.0
60	75	29	Rh	Rh	120.7	2.02	2.61	> 4.5
70	90	30	Rh	Rh	91.6	1.75	2.47	> 6.5

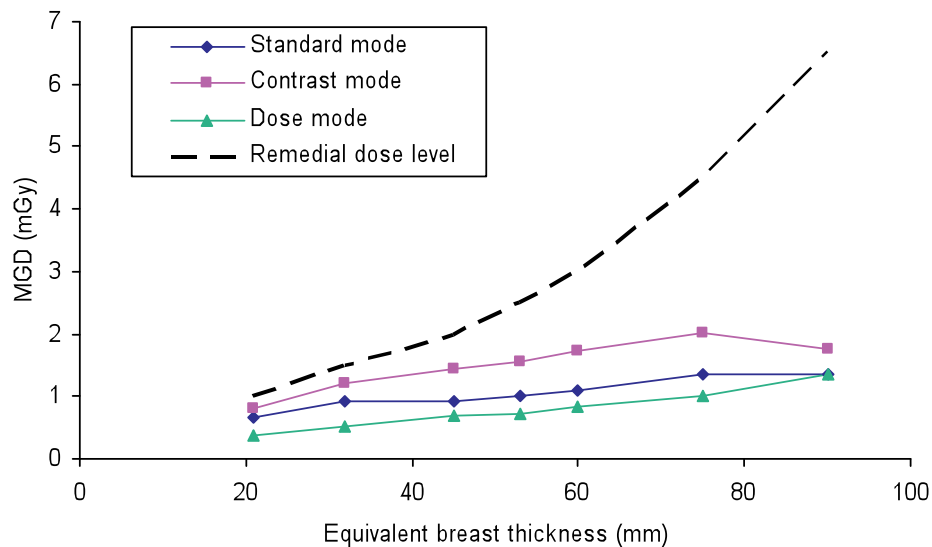


Figure 5 MGD for different thicknesses of simulated breasts using the three AEC modes.

Technical evaluation of the GE Essential FFDM system

3.2.2 CNR

The results of the contrast and CNR measurements are shown in Table 4 and Figure 6. The CNRs required to meet the minimum acceptable and achievable image quality standards at the 60 mm breast thickness have been calculated and are shown in Table 5 and Figure 6. The CNRs required at each thickness to meet the limiting values for CNR in the European protocol are also shown.

Table 5a Contrast and CNR measurements using AEC (standard mode)

Equivalent breast thickness (mm)	kV target/filter	mAs	Back-ground pixel value	% contrast for 0.2 mm Al	Measured CNR	CNR at minimum acceptable IQ	CNR at achievable IQ	CNR to meet European limiting value	European limiting values for relative CNR
21	26 Mo/Mo	25.9	690	21.2	30.2	11.0	16.0	12.6	>115
32	26 Mo/Mo	47.1	587	21.3	25.2	11.0	16.0	12.1	>110
45	29 Rh/Rh	41.1	756	14.9	19.4	11.0	16.0	11.5	>105
53	29 Rh/Rh	48.6	669	14.6	17.5	11.0	16.0	11.3	>103
60	29 Rh/Rh	57.7	599	14.4	16.3	11.0	16.0	11.0	>100
75	29 Rh/Rh	81.3	482	13.9	13.1	11.0	16.0	10.4	>95
90	30 Rh/Rh	81.3	347	13.5	10.0	11.0	16.0	9.9	>90

Table 5b Contrast and CNR measurements using AEC (contrast mode)

Equivalent breast thickness (mm)	kV target /filter	mAs	Back-ground pixel value	% contrast for 0.2 mm Al	Measured CNR	CNR at minimum acceptable IQ	CNR at achievable IQ	CNR to meet European limiting value	European limiting values for relative CNR
21	26 Mo/Mo	31.2	835	21.1	32.8	11.0	16.0	12.6	>115
32	26 Mo/Mo	63.2	792	20.8	30.1	11.0	16.0	12.1	>110
45	29 Rh/Rh	64.2	1186	14.6	23.9	11.0	16.0	11.5	>105
53	29 Rh/Rh	74.9	1039	14.4	22.6	11.0	16.0	11.3	>103
60	29 Rh/Rh	90.7	945	13.9	19.8	11.0	16.0	11.0	>100
75	29 Rh/Rh	120.7	721	13.4	16.7	11.0	16.0	10.4	>95
90	31 Rh/Rh	91.6	485	12.5	11.8	11.0	16.0	9.9	>90

Technical evaluation of the GE Essential FFDM system

Table 5c Contrast and CNR measurements using AEC (dose mode)

Equivalent breast thickness (mm)	kV target/ filter	mAs	Back-ground pixel value	% contrast for 0.2 mm Al	Measured CNR	CNR at minimum acceptable IQ	CNR at achievable IQ	CNR to meet European limiting value	European limiting values for relative CNR
21	27 Mo/Mo	13.0	414	21.2	22.0	11.0	16.0	12.6	>115
32	26 Mo/Mo	27.3	436	19.9	18.6	11.0	16.0	12.1	>110
45	29 Rh/Rh	30.1	549	15.4	16.5	11.0	16.0	11.5	>105
53	29 Rh/Rh	35.4	485	15.2	14.4	11.0	16.0	11.3	>103
60	29 Rh/Rh	44.0	452	15.0	13.6	11.0	16.0	11.0	>100
75	30 Rh/Rh	53.4	388	14.0	11.2	11.0	16.0	10.4	>95
90	30 Rh/Rh	81.6	348	13.5	9.9	11.0	16.0	9.9	>90

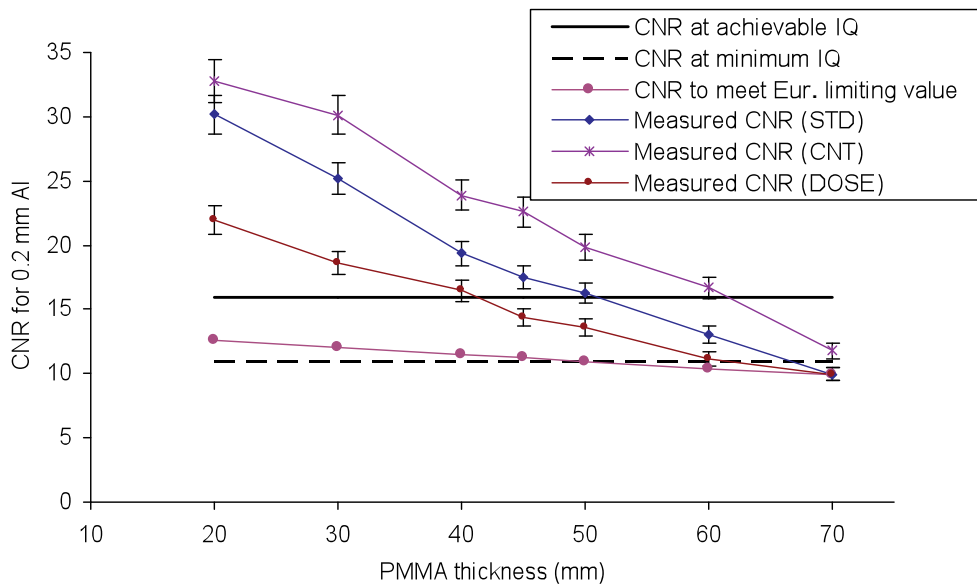


Figure 6 Measured CNR compared with the limiting values in the European protocol for the system (error bars indicate 95% confidence limits).

3.3 Noise measurements

The variation in noise with dose was analysed by plotting the standard deviation in pixel values against the detector entrance air kerma as shown in Figure 7. The fitted power curve has an index of 0.406. If only quantum noise sources were present, the data would form a straight line with an index of 0.5. The presence of some electronic noise and structural noise has caused the curve to deviate from a straight line. This is normal for such systems, and quantum noise was the dominant noise source.

The relative noise is plotted against the background pixel value in Figure 8. The pixel value is proportional to the dose absorbed by the detector. A curve of the form described in equation 5 with an index $n=0.59$ has been fitted to the measured data. A value of n of 0.5 would be expected if only quantum noise were present.

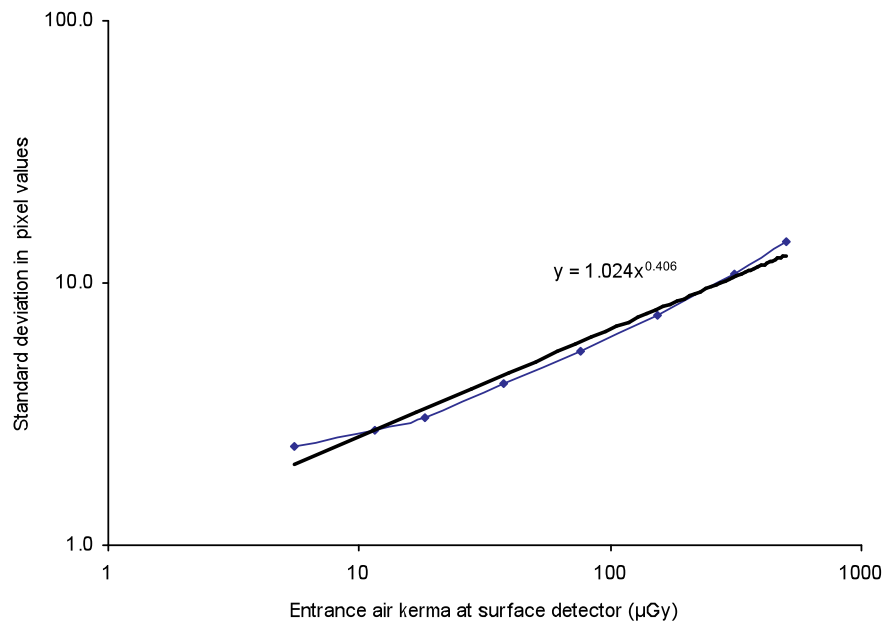


Figure 7 Standard deviation of pixel values versus air kerma at detector.

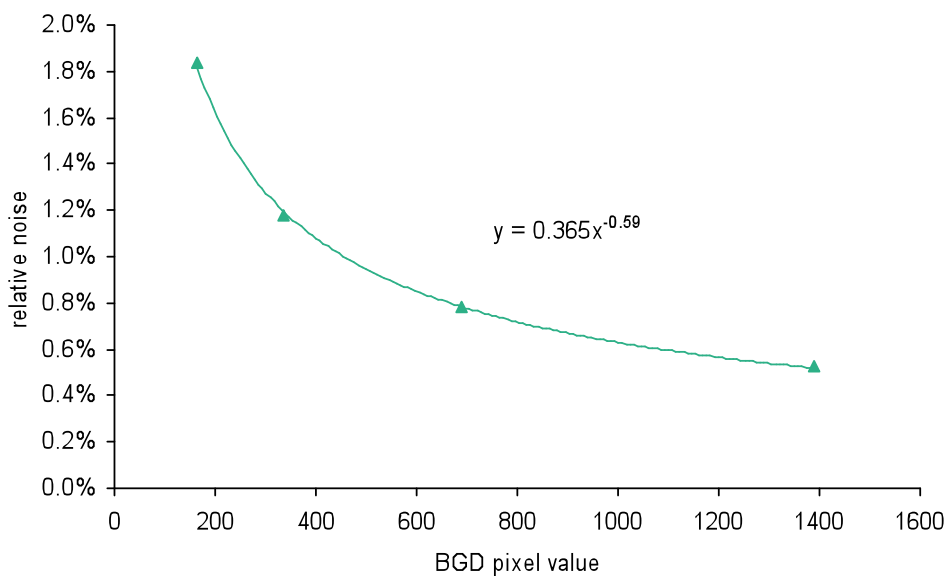


Figure 8 Relative noise at different pixel values.

Figure 9 is an alternative way of presenting the data and shows the relative noise at different average pixel values. The estimated relative contributions of electronic, structural and quantum noise are shown and the quadratic sum of these contributions fitted to the measured noise (using equation 3).

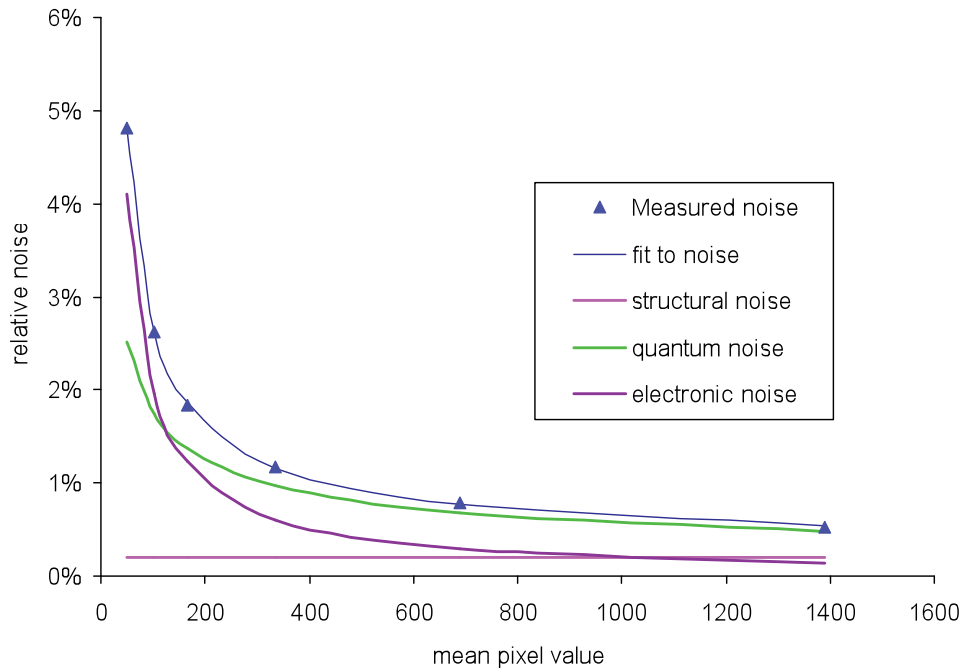


Figure 9 Relative noise and noise components at different pixel values.

3.4 Image quality measurements

The first exposures of the image quality phantom were made using the AEC in standard mode to select the beam quality and exposure factors. This resulted in the selection of 29 kV Rh/Rh and 57.3 mAs and an MGD of 1.06 mGy to an equivalent breast (60 mm thick). Subsequent image quality measurements were made at approximately quarter, half, double and quadruple this dose by manual selection of the mAs at the same beam quality as shown in Table 6.

Table 6 Images acquired for image quality measurement

Exposure mode	kV target/filter	mAs	Mean glandular dose to equivalent breasts 60 mm thick (mGy)	Number of CDMAM images acquired and analysed
Manual	29 Rh/Rh	14	0.26	12
Manual	29 Rh/Rh	28	0.52	16
AEC (standard dose)	29 Rh/Rh	57.3	1.06	16
Manual	29 Rh/Rh	110	2.04	16
Manual	29 Rh/Rh	225	4.16	16

Technical evaluation of the GE Essential FFDM system

The contrast detail curves at the five dose levels are shown in Figure 10. The threshold gold thicknesses for different diameters and the five different dose levels for this system are shown in Table 7, along with the minimum and achievable threshold values from the NHSBSP protocol (ie same as the European protocol). The data in Table 7 are taken from the fitted curves rather than the raw data.

The measured threshold gold thicknesses are plotted against the MGD for an equivalent breast for the 0.1 and 0.25 mm detail sizes in Figure 11. This shows how the threshold gold thickness reduced as the dose was increased. The fitted curves such as shown in Figure 11 were used to determine the doses required to meet the minimum acceptable and achievable image quality levels for detail sizes from 0.1 to 1.0 mm and are shown in Figure 12.

Table 7a Average threshold gold thicknesses for different detail diameters for five different doses using 29 kV Rh/Rh and human data. Data are interpolated using curve fits

Diameter (mm)	Threshold gold thickness (µm)						
	Acceptable value	Achievable value	MGD = 0.26 mGy	MGD = 0.52 mGy	MGD = 1.06 mGy	MGD = 2.04 mGy	MGD = 4.16 mGy
0.1	1.680	1.100		2.089 ± 0.209	1.360 ± 0.136	1.108 ± 0.111	0.732 ± 0.073
0.25	0.352	0.244	0.541 ± 0.054	0.353 ± 0.035	0.262 ± 0.026	0.180 ± 0.018	0.131 ± 0.013
0.5	0.150	0.103	0.206 ± 0.021	0.154 ± 0.015	0.109 ± 0.011	0.079 ± 0.008	0.060 ± 0.006
1	0.091	0.056	0.105 ± 0.010	0.081 ± 0.008	0.056 ± 0.006	0.044 ± 0.004	0.038 ± 0.004

Table 7b Average threshold gold thicknesses for different detail diameters for five different doses using 29 kV Rh/Rh and automatically predicted data. Data are interpolated using curve fits

Diameter (mm)	Threshold gold thickness (µm)						
	Acceptable value	Achievable value	MGD = 0.26 mGy	MGD = 0.52 mGy	MGD = 1.06 mGy	MGD = 2.04 mGy	MGD = 4.16 mGy
0.1	1.680	1.100	2.643 ± 0.394	1.857 ± 0.186	1.080 ± 0.108	0.657 ± 0.066	0.552 ± 0.055
0.25	0.352	0.244	0.505 ± 0.041	0.341 ± 0.017	0.230 ± 0.011	0.173 ± 0.008	0.120 ± 0.006
0.5	0.150	0.103	0.211 ± 0.018	0.147 ± 0.008	0.094 ± 0.005	0.073 ± 0.004	0.057 ± 0.003
1	0.091	0.056	0.105 ± 0.013	0.079 ± 0.006	0.054 ± 0.004	0.037 ± 0.003	0.034 ± 0.003

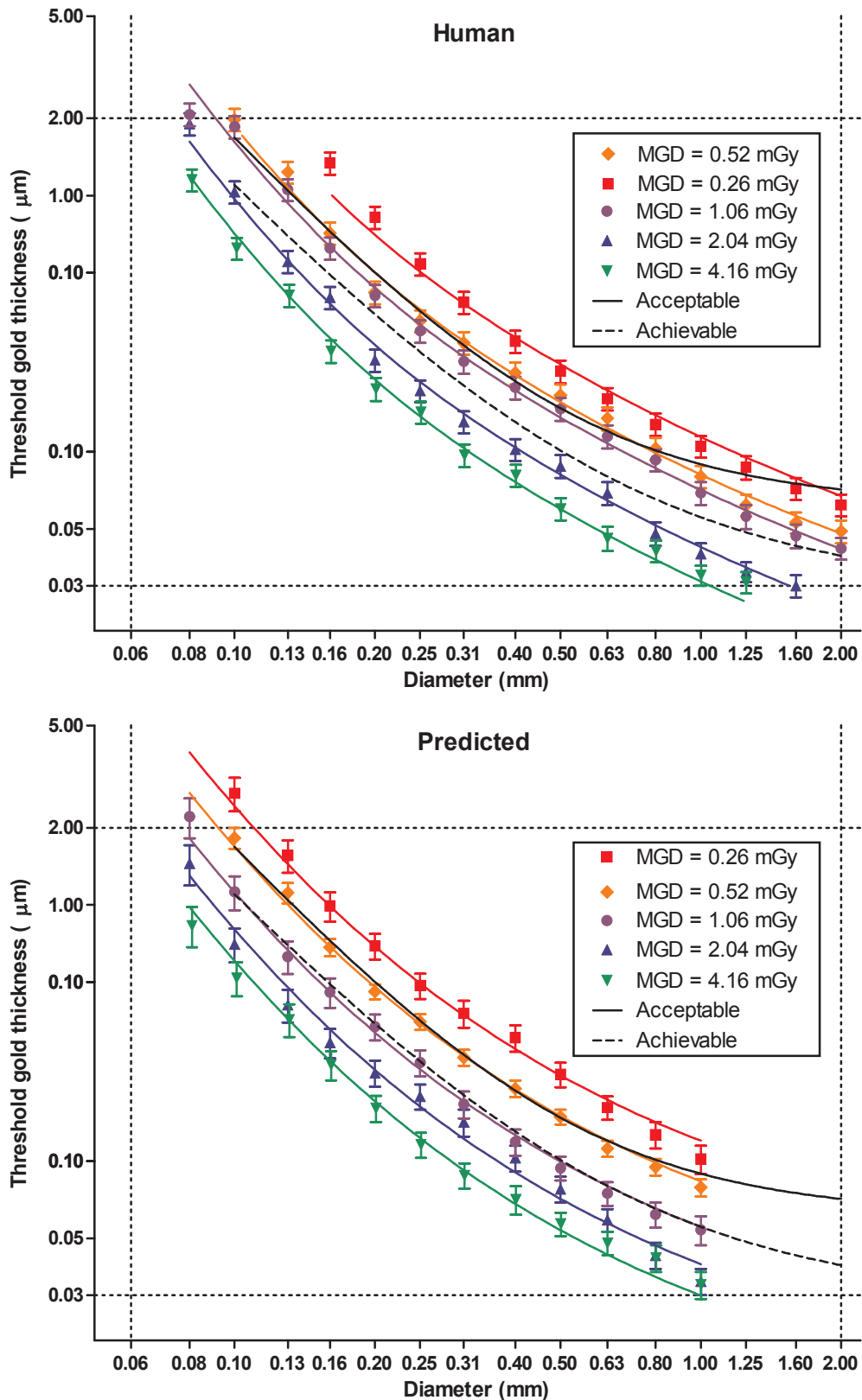


Figure 10 Contrast–detail curves for the system for five different doses at 29 kV Rh/Rh using human and predicted results from automated reading. The 1.06 mGy dose corresponds to the AEC selection in standard mode. Error bars indicate 95% confidence limits.

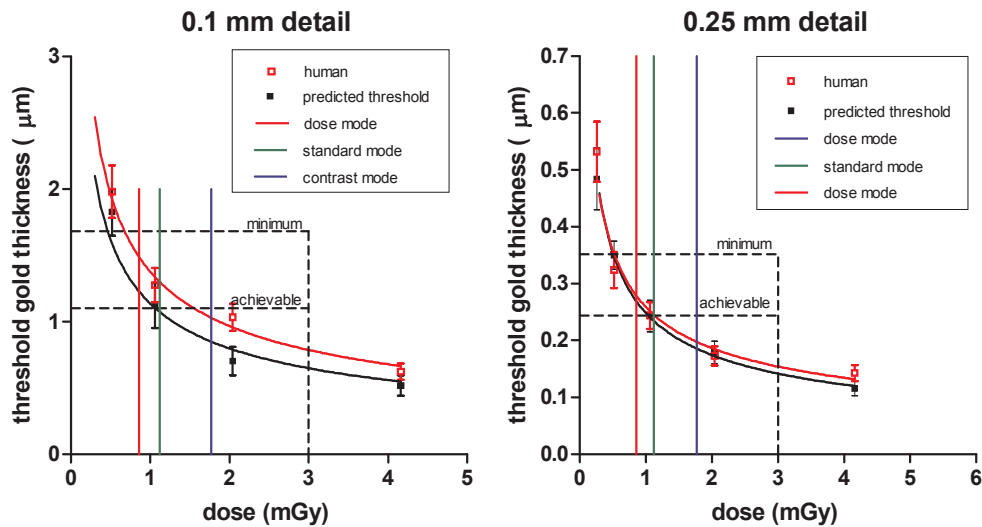


Figure 11 Threshold gold thickness at different doses. Error bars indicate 95% confidence limits. The doses selected for a 5 cm thickness of PMMA using the three AEC dose modes are shown by the coloured vertical lines.

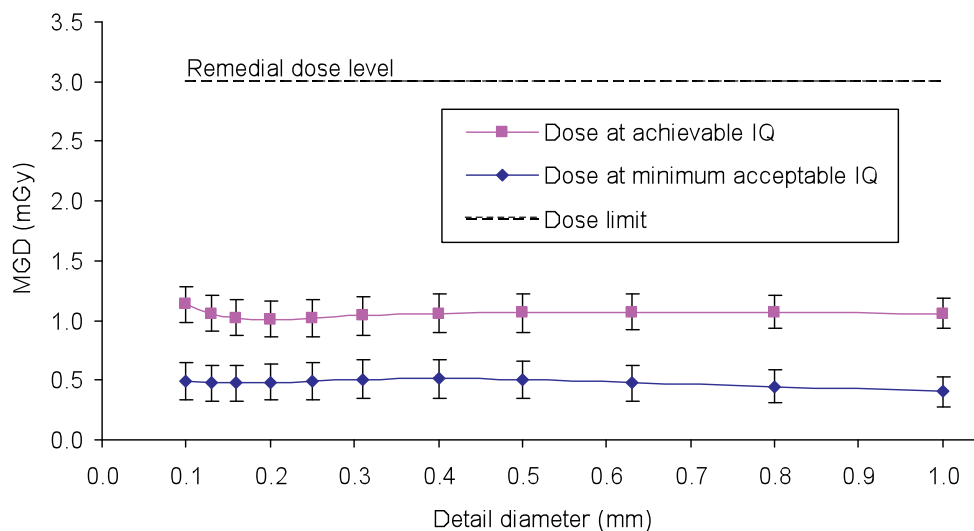


Figure 12 The MGD calculated to be necessary to reach the achievable and minimum acceptable image quality levels at different detail sizes using 29 kV Rh/Rh for an equivalent breast 60 mm thick. Based on predicted threshold gold thicknesses.

3.5 Comparison with other systems

The MGDs to reach the minimum and achievable image quality standards in the NHSBSP protocol have been estimated from the curves shown in Figure 11. (The error in estimating these doses depends on the accuracy of the curve fitting procedure, and pooled data for several systems has been used here to estimate the 95% confidence limits of about 20%.) These doses are shown against similar data for other models of digital mammography system in Tables 8 and 9 and Figures 13 to 16. The data for the other systems have been determined in the same way as described in this report and the results published previously.⁶⁻¹¹ The data for film-screens represent an average value determined using a variety of modern film-screen systems.

Technical evaluation of the GE Essential FFDM system

Table 8 The MGD for different systems to reach the minimum threshold gold thickness for 0.1 and 0.25 mm details

System	MGD (mGy) for 0.1 mm		MGD (mGy) for 0.25 mm	
	Human	Predicted	Human	Predicted
Fischer Senoscan	0.55	0.42	0.48	0.53
Sectra MDM	0.60	0.82	0.67	0.46
Siemens Novation ^a	0.63	0.61	0.52	0.63
Siemens Novation ^b	0.44	0.56	0.41	0.71
Hologic Selenia (Mo)	0.85	0.55	0.80	0.53
Hologic Selenia (W)	0.58	0.71	0.65	0.64
GE Essential	0.60	0.49	0.50	0.49
GE DS	1.01	0.82	0.87	0.83
Film-screen	1.17	1.30	1.07	1.36
Fuji Profect CR	1.67	1.78	1.45	1.35
Agfa CR 85-X	2.00	1.94	0.86	1.42
Kodak CR (EHR-M2)	2.29	2.34	1.45	1.80
Kodak CR (EHR-M)	3.46	2.49	1.49	1.33
Test CR	4.52	4.17	2.33	2.12

^aSystem at Erlangen.

^bSystem at Cambridge.

Table 9 The MGD for different systems to reach the achievable threshold gold thickness for 0.1 and 0.25 mm details

System	MGD (mGy) for 0.1 mm		MGD (mGy) for 0.25 mm	
	Human	Predicted	Human	Predicted
Fischer Senoscan	1.16	0.90	0.98	1.09
Sectra MDM	1.27	1.74	1.37	0.95
Siemens Novation ^a	1.56	1.21	1.14	1.27
Siemens Novation ^b	1.03	1.30	0.85	1.47
Hologic Selenia (Mo)	1.84	1.19	1.68	1.12
Hologic Selenia (W)	1.66	1.37	1.61	1.48
GE Essential	1.57	1.13	1.14	1.03
GE DS	2.35	1.57	1.80	1.87
Film-screen	2.48	3.03	2.19	2.83
Fuji Profect CR	4.26	3.29	3.52	2.65
Agfa CR 85-X	5.03	4.88	2.20	3.15
Kodak CR (EHR-M2)	5.34	5.45	3.03	3.74
Kodak CR (EHR-M)	7.74	5.56	6.28	5.60
Test CR	11.5	9.90	5.96	5.63

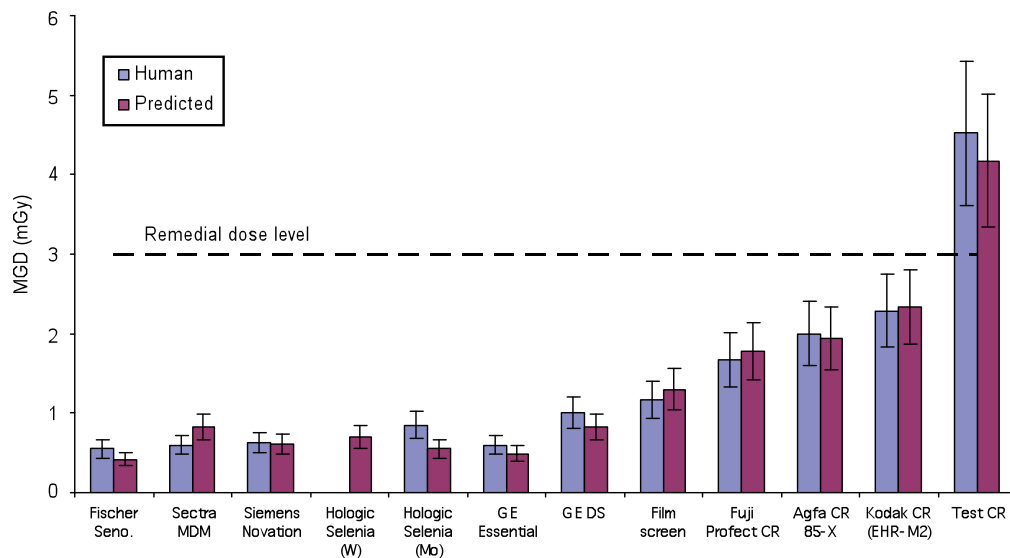


Figure 13 Dose to reach minimum acceptable image quality standard for 0.1 mm detail. Error bars indicate 95% confidence limits.

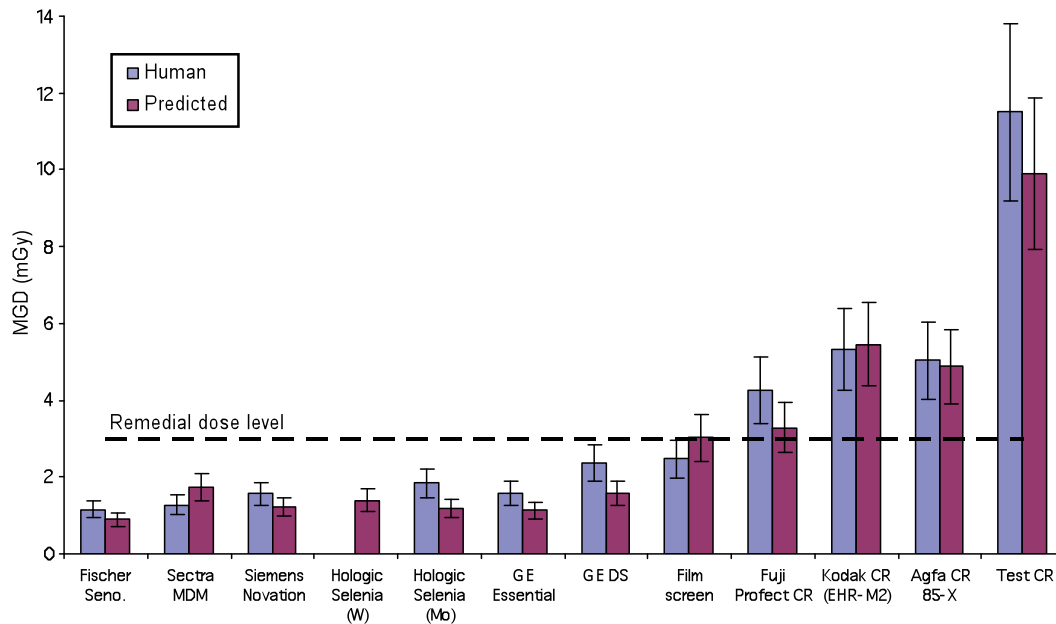


Figure 14 Dose to reach achievable image quality standard for 0.1 mm detail. Error bars indicate 95% confidence limits.

Technical evaluation of the GE Essential FFDM system

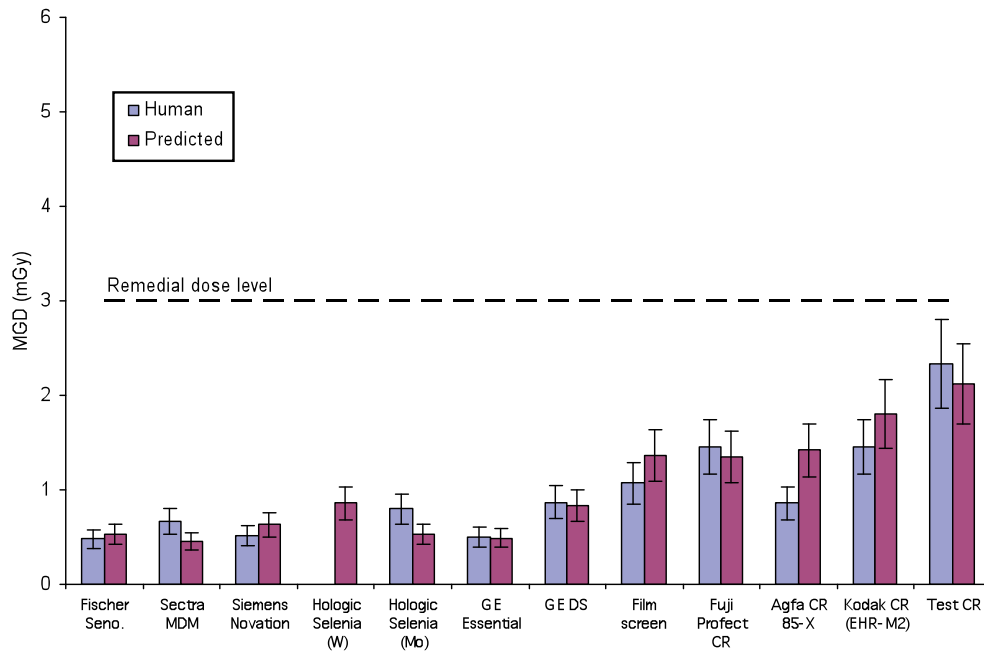


Figure 15 Dose to reach minimum acceptable image quality standard for 0.25 mm detail. Error bars indicate 95% confidence limits.

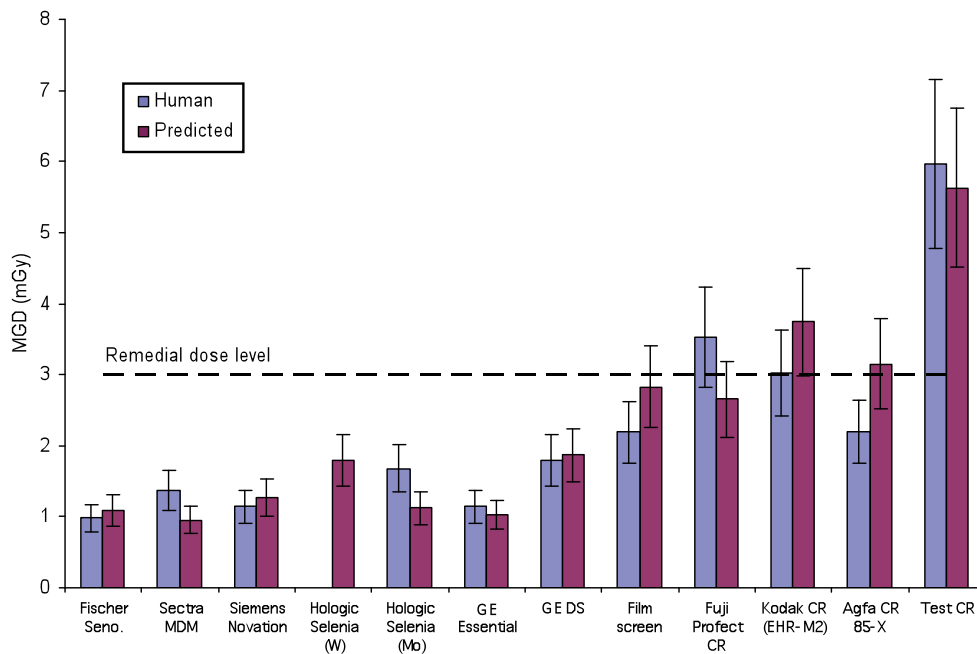


Figure 16 Dose to reach achievable image quality standard for 0.25 mm detail. Error bars indicate 95% confidence limits.

3.6 Optimisation

The target CNR corresponding to the achievable image quality standard was calculated to be 16.0. The MGDs required to reach this target CNR for each beam quality and thickness of PMMA are shown in Figure 17. From these data the optimal beam qualities and mAs were calculated and are shown in Table 10. Table 11 shows a similar calculation using the kV/target/filter combinations selected by the AEC in standard mode along with the mAs necessary to achieve a CNR of 16.0.

Table 10 Optimal factors to reach achievable image quality (ie where CNR=16.0) at the lowest dose

PMMA thickness	kV target/filter	Background pixel value	mAs	MGD (mGy)	Dose compared to standard mode AEC selection (%)	Remedial dose level in NHSBSP protocol (mGy)
20	28 Mo/Mo	229	6	0.20	31	1.0
30	28 Rh/Rh	412	15	0.37	40	1.5
40	31 Rh/Rh	564	21	0.62	67	2.0
45	28 Rh/Rh	506	45	0.82	81	2.5
50	28 Rh/Rh	512	61	1.02	92	3.0
60	31 Rh/Rh	793	88	1.92	141	4.5
70	31 Rh/Rh	899	167	3.19	237	6.5

Table 11 Settings required to reach achievable image quality (ie CNR=16.0) using the beam quality selections made by the AEC in standard dose mode

PMMA thickness	kV target/filter	Background pixel value	mAs	MGD (mGy)	Dose saving if optimal beam quality used (%)	Remedial dose level in NHSBSP protocol (mGy)
20	26 Mo/Mo	199	7	0.19	-7	1.0
30	26 Mo/Mo	225	19	0.37	2	1.5
40	29 Rh/Rh	494	28	0.64	3	2.0
45	29 Rh/Rh	529	41	0.84	3	2.5
50	29 Rh/Rh	543	56	1.07	5	3.0
60	29 Rh/Rh	661	121	2.03	5	4.5
70	30 Rh/Rh	779	206	3.41	6	6.5

Technical evaluation of the GE Essential FFDM system

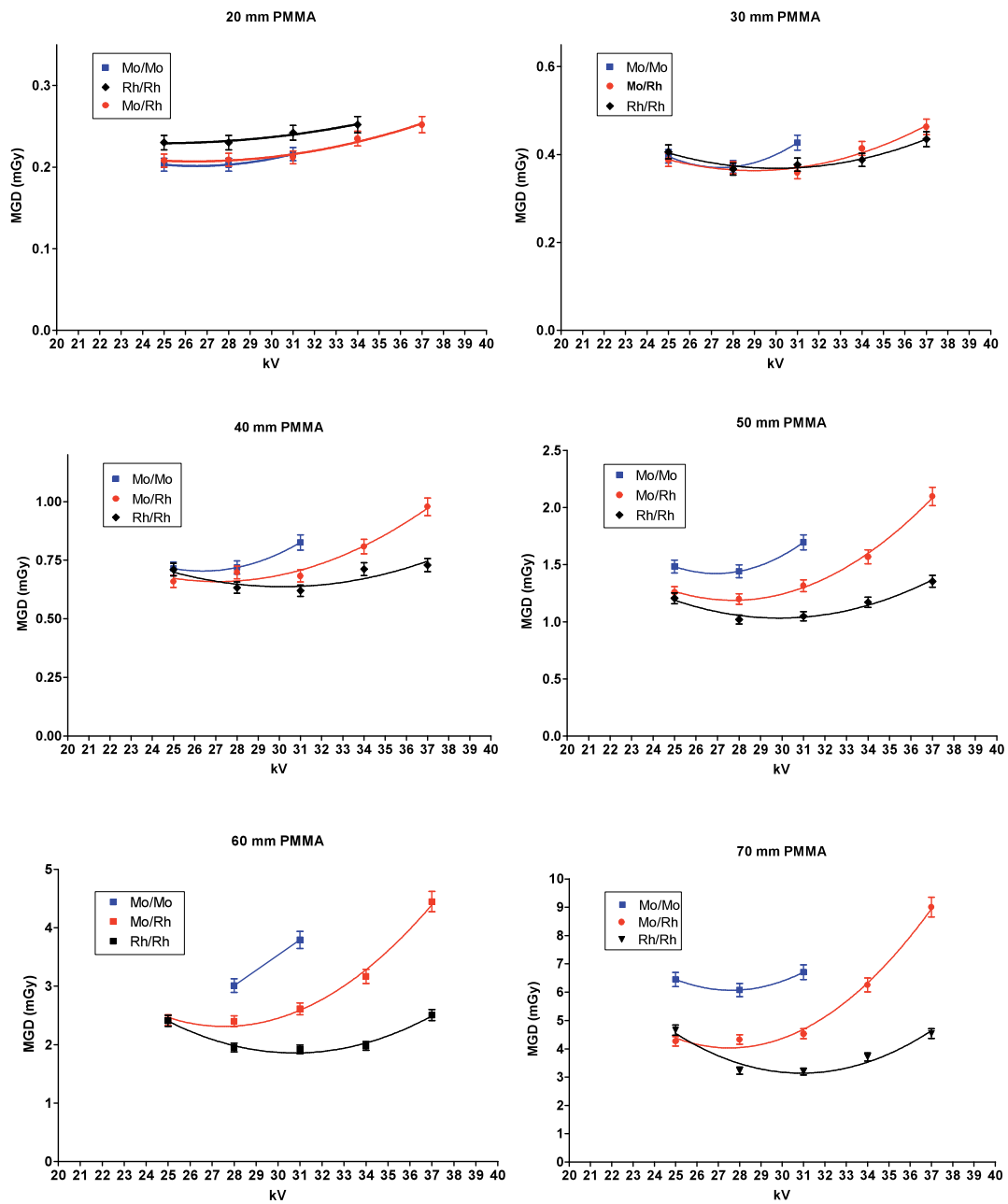


Figure 17 MGD to reach the achievable image quality standard in the NHSBSP protocol (ie CNR = 16.0). Error bars indicate 95% confidence limits.

4. DISCUSSION

The detector response was, as expected, linear with no pixel value offset. The noise analysis confirmed that quantum noise is the dominant noise source. As with most systems, there was also evidence of some electronic and structural noise. In all three dose modes the AEC resulted in doses to simulated breasts that were well below the limits in the NHSBSP protocol. The doses for the standard breast simulated with 45 mm of PMMA in the three modes were 1.55, 1.10 and 0.73 mGy. At this thickness an upper limit of 2.5 mGy is applied by the NHSBSP. The doses calculated and displayed by the system itself were higher than calculated by us. The reason for these differences is not clear.

The three AEC modes resulted in background pixel values that varied between 350 and 1200 depending on the thickness and the mode used. The AEC chose the Rh/Rh target/filter combination for simulated breast thicknesses of 45 mm and greater with a tube voltage in the range 29–31 kV. The Mo/Mo combination was selected for lower thicknesses with a 26 or 27 kV tube voltage. The net result of these choices was that the CNR values were relatively high for thinner breasts but dropped steeply with increasing breast thickness. All three AEC modes exceeded the minimum requirements in the European protocol. However, the CNR values seemed much higher than necessary for the thinner breasts, but fell well below that necessary to reach the achievable level of image quality for the largest simulated thicknesses. At all settings the minimum acceptable CNR value was met or exceeded. A feature of the AEC not tested by the current protocols is the increase in exposure when dense tissue is detected. It is expected that, in practice, this will result in higher doses and higher image quality than expected from testing with uniform blocks of PMMA.

The image quality measurements indicated that for the standard thickness tested (equivalent to 50 mm thickness of PMMA, ie 60 mm of typical breast) the image quality was close to the achievable level in standard mode. In this mode the AEC selected a dose of 1.10 mGy using 29 kV Rh/Rh. Figure 11 shows that the use of the dose mode will result in an image quality slightly below the achievable level, at a dose of 0.83 mGy. The use of the contrast mode resulted in a dose of 1.74 mGy, and an image quality better than the achievable standard. A dose of about 0.49 ± 0.15 mGy was calculated to be necessary to reach the minimum image quality level for this equivalent breast thickness. A dose of about 1.10 ± 0.15 mGy was calculated to be necessary to reach the achievable image quality level for this equivalent breast thickness.

The doses required to reach the acceptable and achievable image quality levels are lower than reported previously for the Senographe DS models. Presumably this is explained by the improvements in efficiency with the Essential design. The doses at the two image quality levels are broadly similar to those of the other DR systems so far tested.

The optimisation study demonstrated that the current beam qualities chosen by the AEC are close to optimal. The calculated optimal kV/target/filter combinations shown in Table achieved 9 only modest dose savings (<10%) compared with the doses shown in Table 10 where the current AEC selections were used. However the mAs and background pixel values seem too high for small breasts and too low for the thickest breasts. This could be overcome by selecting the contrast mode for the greater thicknesses of compressed breast (ie greater than 60 mm thick.)

5. CONCLUSIONS

This system is capable of producing excellent image quality for a relatively low radiation dose. As currently set up, the AEC will be satisfactory for most types of breast in all three AEC modes. It is expected that the standard mode will be suitable for most applications, but contrast mode may be preferable for the largest breasts. The system met the main standards in the NHSBSP and European protocols and seems to represent an improvement over previous models from the same manufacturer in terms of image quality and/or dose efficiency.

6. MANUFACTURER'S COMMENT

The results shown in this report relate to the use of the system with the original AOP tables which we now call 'CLASSIC'. We plan to introduce a second set of AOP tables that we call 'PROFILE'. The main change is that the new tables will achieve a higher CNR for the largest breasts at the expense of a slightly higher dose. (It is expected that these new tables will be the subject of a later addendum to this report.)

REFERENCES

1. Workman A, Castellano I, Kulama E, Lawinski CP, Marshall N, Young KC. *Commissioning and Routine Testing of Full Field Digital Mammography Systems*. NHS Cancer Screening Programmes, 2006 (NHSBSP Equipment Report 0604).
2. Young KC, Johnson B, Bosmans H, Van Engen R. Development of minimum standards for image quality and dose in digital mammography. In *Digital Mammography*, 2005 (IWDM 2004, Proceedings of the Workshop in Durham NC, USA, June 2004).
3. Van Engen R, Young KC, Bosmans H, Thijssen M. The European protocol for the quality control of the physical and technical aspects of mammography screening. In: *European Guidelines for Breast Cancer Screening*, 4th edn. Luxembourg: European Commission, 2006.
4. Young KC, Cook JJH, Oduko JM. Use of the European protocol to optimise a digital mammography system. In: Astley SM, Bradey M, Rose C, Zwigelaar R, eds. Proceedings of the 8th International Workshop on Digital Mammography. *Lecture Notes in Computer Science*, 2006, 4046: 362–369.
5. Young KC, Oduko JM, Bosmans H, Nijs K, Martinez L. Optimal beam quality selection in digital mammography. *British Journal of Radiology*, 2006, 79: 981–990.
6. Young KC, Cook JJH, Oduko JM, Bosmans H. Comparison of software and human observers in reading images of the CDMAM test object to assess digital mammography systems. *Proceedings of SPIE Medical Imaging*, 2006, 614206: 1–13.
7. Young KC, Cook JJH, Oduko JM. Automated and human determination of threshold contrast for digital mammography systems. In: Astley SM, Bradey M, Rose C, Zwigelaar R, eds. Proceedings of the 8th International Workshop on Digital Mammography. *Lecture Notes in Computer Science*, 2006, 4046: 266–272.
8. Young KC, Alsager A, Oduko JM, Bosmans H, Verbrugge B, Geertse T, Van Engen R. Evaluation of software for reading images of the CDMAM test object to assess digital mammography systems. *Proceedings of SPIE Medical Imaging*, 2008, 69131C, 1–11.
9. Young KC, Oduko JM. *Evaluation of Kodak DirectView Mammography Computerised Radiography*. NHS Cancer Screening Programmes, 2005 (NHSBSP Equipment Report 0504).
10. Young KC, Oduko JM, Woolley L. *Technical Evaluation of the Hologic Selenia Full Field Digital Mammography System*. NHS Cancer Screening programmes, 2007 (NHSBSP Equipment Report 0701).

11. Young KC, Oduko JM. *Technical Evaluation of Kodak DirectView Mammography Computerised Radiography System using EHR-M2 Plates*. NHS Cancer Screening Programmes, 2007 (NHSBSP Equipment Report 0706).
12. Young KC, Oduko JM. *Technical Evaluation of Agfa CR-85 Mammography System*. NHS Cancer Screening programmes, 2007 (NHSBSP Equipment Report 0707).
13. Young KC, Oduko JM. *Technical Evaluation of the Hologic Selenia Full Field Digital Mammography System with a Tungsten Tube*. NHS Cancer Screening Programmes, 2008 (NHSBSP Equipment Report 0801).